DOI: 10.21062/mft.2024.089 http://www.journalmt.com

Numerical Simulation of a Cylindrical Outer Flanging Spinning

Xuhui Yang (0009-0006-5724-5588)[1,2], Zhen Jia (0000-0002-2433-641X)[1]
[1]School of Aerospace Engineering, Shenyang Aerospace University, Shenyang 110136, China. E-mail: jiaz_2006@sina.com
[2]Elite Engineers School, Harbin Institute of Technology, Harbin 150001, China. E-mail: yxh17541162810@163.com

The use of spinning technology for the outer flanging of cylindrical parts can save molds, reduce labor intensity, and improve production efficiency. Therefore, two finite element models for the outer flanging spinning with the flange radius of 4 mm and 5 mm are established in this article. And the deformation process, stress-strain field, and wall thickness distribution of the flange during the spinning period are analyzed. It can be found from the simulation results that, the blank of both working conditions cannot fit the contour of the roller until the until 2.5 s before the end of the spinning process, and it is more difficult to achieve fitting with a smaller profiling radius of 4 mm. The x-direction force caused by the 4mm profiling radius is less than that by the 5 mm one before the end of forming due to the smaller contact area with the roller. According to deformation in a relatively cramped area, the wall thickness distribution under the condition with larger curvature are generally slightly greater than that with smaller one.

Keywords: Cylindrical thin-wall part, Flanging spinning; Numerical simulation, Metal flow, Contour fit degree

1 Introduction

Cylindrical thin-wall parts are commonly used in aviation, transportation and agricultural machinery fields. And some cylindrical shells require flanging on the end. Traditional manual flanging has the disadvantages of high labor intensity, poor working environment and low manufacturing accuracy. Die forming can overcome the above defects, but a pair of concave-convex dies need to be processed, increasing the processing cost and delaying the production cycle. Spinning is an efficient and material-saving metal forming process, which can replace one of the concave-convex dies with the roller[1-3], hence the the production preparation cycle and cost of the flanging process will be reduced.

Yuan et al [4] adopted the flanging spinning in the manufacture of a large slenderness ratio cylinder with multi diameters, and achieved the inner flanging at the cylindrical end. Ball spinning was used to form the flange hole by He and Huang [5, 6]. They analyzed the effects of feed rate, ball diameter and thinning rate on the ball spinning force as well as the stress and strain distribution though finite element simulation. Xu et al [7] designed the die device for the hot flanging spinning of titanium alloy wheel rim according to its structure characteristics. They analyzed the forming defects of titanium alloy hot spinning process and found the split combined die is a reasonable structure scheme. Meanwhile, the forming quality of the titanium alloy wheel rim is influenced by the hot spinning parameters (such as forming temperature, feed rate and roller gap, etc) significantly. A fanged bushing was manufactured using power spinning by Bai [8], they analyzed the characteristics and difficulties of the process, and obtained the theoretical values of the process dimensions which meet the production demands through simulation and calculation. Zhao et al. [9] introduced a new engine cylinder liner flanging process with the design of specialized fixture and the spinning tools.

The above researches introduce several flanging spinning processes, explain the influence of processing parameters on forming accuracy, introduce specialized equipment, and and analyze the metal flow field of ball flanging spinning by using finite element modeling, providing reference experience for the research of outer flanging spinning of cylindrical parts. However, the stress-strain and metal flow history during the outer flanging spinning of parts has significant uniqueness, and further investigation is needed due to its imitative profiling roller. The numerical simulation study can effectively solve the key problems during the spinning experiment. For example, Jia et al [10] simulated the non-axisymmetric die-less shear spinning process, and showed that the equivalent strain-stress distributions also present asymmetric state. The multi-pass non-axisymmetric tube necking spinning was carried out by Xia et al. [11] using the MARC software. And They got the stress and strain fields of the non-axisymmetric tubular end. Sui et al [12] established analyzed the metal flow of the cylinder closure spinning

using finite element modeling. The multi-pass non-axisymmetric spinning of cylindrical parts with oblique flange was simulated by Ye et al [13] to describe relationship between the forming parameters and the shape accuracy. Jia et al [14, 15] investigated the effects of the processing parameters on the surface quality, stress-strain fields of the square section die-less spinning by using the finite element modeling.

The efficient development of spinning technology is closely related to finite element methods. Finite element technology can achieve real-time acquisition of information such as forming force, stress-strain fields, and cross-sectional contour fit degree during the spinning process. Therefore, a finite element model for the outer flange spinning of cylindrical parts is established in this study, and the simulation result is analyzed to provide a theoretical basis for actual production.

2 Establishment of the simulation model

According to the production demand, the finite element modeling process of the cylindrical outer flanging spinning is established and carried out using the Abaqus software. The 3D geometric models of the cylindrical blank and the profiling roller are established respectively and assembled into a spinning system as shown in Fig.1. The deformable solid body is assigned to the cylindrical blank, as well as, the profiling roller is constrained as the rigid body. The blank and the roller have rotating axes separately (see Fig.1). The profiling roller can rotate around its rotating axis freely and move along this direction (direction Z in Fig.1). However, the cylindrical blank can only rotate at a constant speed of 240r.min^{-1}. The friction coefficient between the blank and the roller is set to be 0.2 according to the production experience, and the roller will be driven to rotate by the friction during the spinning process. The element for the cylindrical blank is meshed as "C3D8R" which is interpreted as 8-node linear brick, reduced integration and hourglass control.

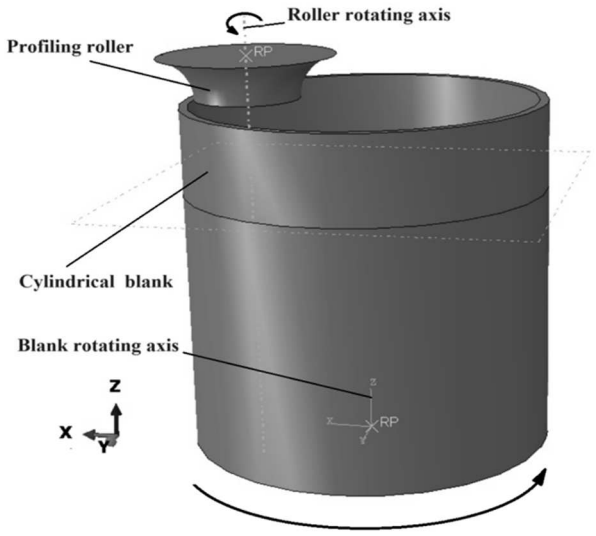

Fig. 1 *3D model of cylindrical outer flanging spinning*

6061O aluminum alloy is selected for the material of the cylindrical blank with the outer diameter of 40mm, 1mm thickness and 40mm height. The material properties of 6061O aluminum alloy is shown in Table 1. And Eq. 1 expresses the plastic stress-strain relationship of the material using in the finite element model [11].

Tab. 1 *Material properties of 6061O aluminum alloy*

Density g.mm^{-3}	Elastic modulus MPa	Poisson ratio	Yield strength MPa	Elongation rate %
2.7	67000	0.33	51.59	25

$$\sigma = 234\varepsilon^{0.26} \quad (1)$$

Where:

σ…True stress [MPa],

ε…True strain [-].

The geometric parameters of the profiling roller are displayed in Fig.2. The height of the roller (H in Fig.2) is 5 mm, the bottom diameter (D_p in Fig.2) is 11.8 mm. Two values of 4mm and 5mm are adopted as the radius of the profiling arc (R_p in Fig.2) in the modeling. And the top diameter of roller dynamically changes with R_p. The moving path of roller is a line along the negative direction of the Z-axis in Fig.1. And the displacement of the roller path is 7 mm for both working conditions with the profiling radii R_p of 4 mm and 5 mm. The feed rate for both spinning conditions is 0.25 mm.r^{-1}. The finite element models of the cylindrical outer flanging spinning are run with all the above boundary conditions.

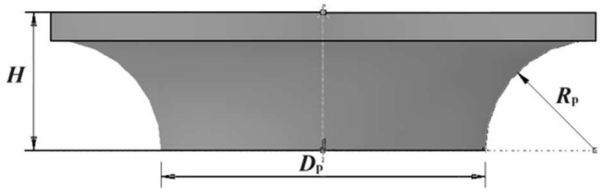

Fig. 2 *3D model of cylindrical outer flanging spinning*

3 Simulation results and analysis

3.1 Deformation process

Fig.3 shows the cylindrical outer flanging spinning process with the roller profiling radius of 4 mm and 5 mm at the time of 2.8 s, 5.6 s and 6.3 s. It can be found that, the lower part of the roller comes into contact with the cylindrical blank, and the material begins to flow outward during the initial spinning stage. At this time, whether in the working condition with the 4mm-

radius roller or the 5 mm one, the inner wall of the blank cannot fit with the outer contour of the roller. When the spinning stroke is completed by 5.6mm which is calculated by multiplying the feed rate (0.25 mm.r^{-1}) by the blank rotating speed (4 r.s^{-1}) and spinning time (5.6 s), the blank material is basically in line with the larger radius contour, however, a small gap still exists between the outward curved contour of the blank and the roller with the 4mm-radius profile. Both working conditions have better contour fit between the roller and the blank after the spinning time reaches 6.3 s. The above spinning modeling results illustrate that the larger the radius, the easier it is for the outer flange to fit the profiling roller, which means that the larger the radius, the easier it is for the outer flange to be spun; Under the premise of sufficient roller pressure distance, the outer flanging spinning with a flanging radius of 4mm is feasible.

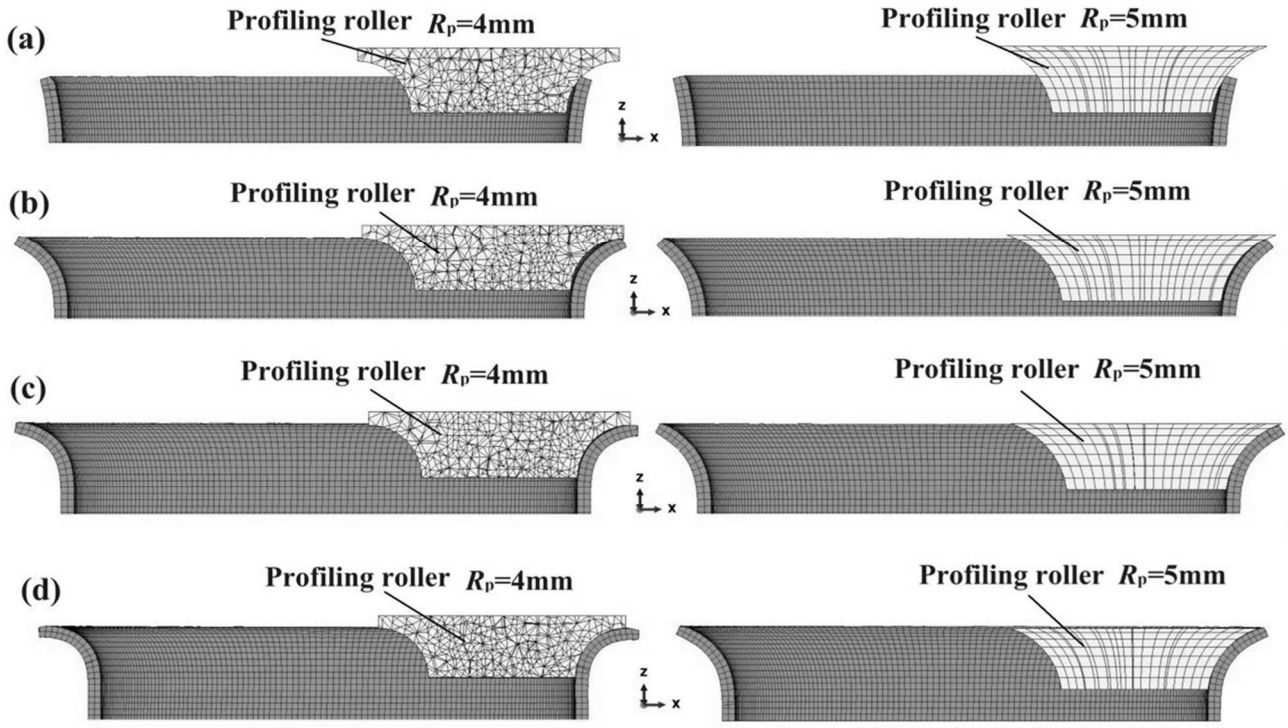

Fig. 3 *Cylindrical outer flanging spinning process with the roller profiling radius of 4mm and 5mm at the time of (a) 2.8s, (b) 5.6s, (c) 6.3s and 7s*

3.2 Stress and spinning force

The distributions of Mises stress on the deforming part during the outer flanging spinning proces are shown in Fig.4. The stress cloud displays that the largest Mises stress appears at the top part of the Cylindrical blank which has the biggest outward flange for both working conditions with the profiling radius of 4 mm and 5 mm. At the spinning time of 2.8 s, the roller with bigger profiling radius causes almost the same Mises stress at deformation zone to that with the smaller one. And then a little bigger Mises stress distribution region appears on the workpiece spun by larger profiling radii at 5.6 s due to the longer Z-direction contacting zone between the roller and the blank. Though the curvature of the roller with the radius of 4mm is bigger than that of 5mm, the contacting gap doesn't cause the material to deform according to the size of the profiling curvature, resulting in the phenomenon of larger stress distribution in working conditions with smaller curvature. At the end of spinning, the workpiece with larger flanging curvature have higher Mises stress due to its greater deformation on direction X and Z.

The roller pushes the metal along the direction X, at the same time the material is pressed at the direction Z to form the outer flange. When the roller applies force to the blank, it also receives a reaction force from the material, which is equal in magnitude and opposite in direction. Fig. 5 shows the X-direction reaction force during the spinning process which is key force in flanging forming. The two working conditions have the consistent overall trend of the X-direction force, with a slight fluctuation and growth before 6.3 s, and a sudden significant increase from 6.3 s to the end of the forming process. The working condition with a contour radius of 4mm on the roller has a larger curvature, and the ability of the blank material to adhere to the roller is weaker before 6 s. Therefore the X-direction force caused by the profiling radius of 4 mm is smaller than that of 5 mm. During the 6.3 s-7s time period, after the two rollers fully adhered to the blank, the X-direction force under the 4mm working condition suddenly exceeded the 5 mm one, which is consistent with the status of Mises stress distribution.

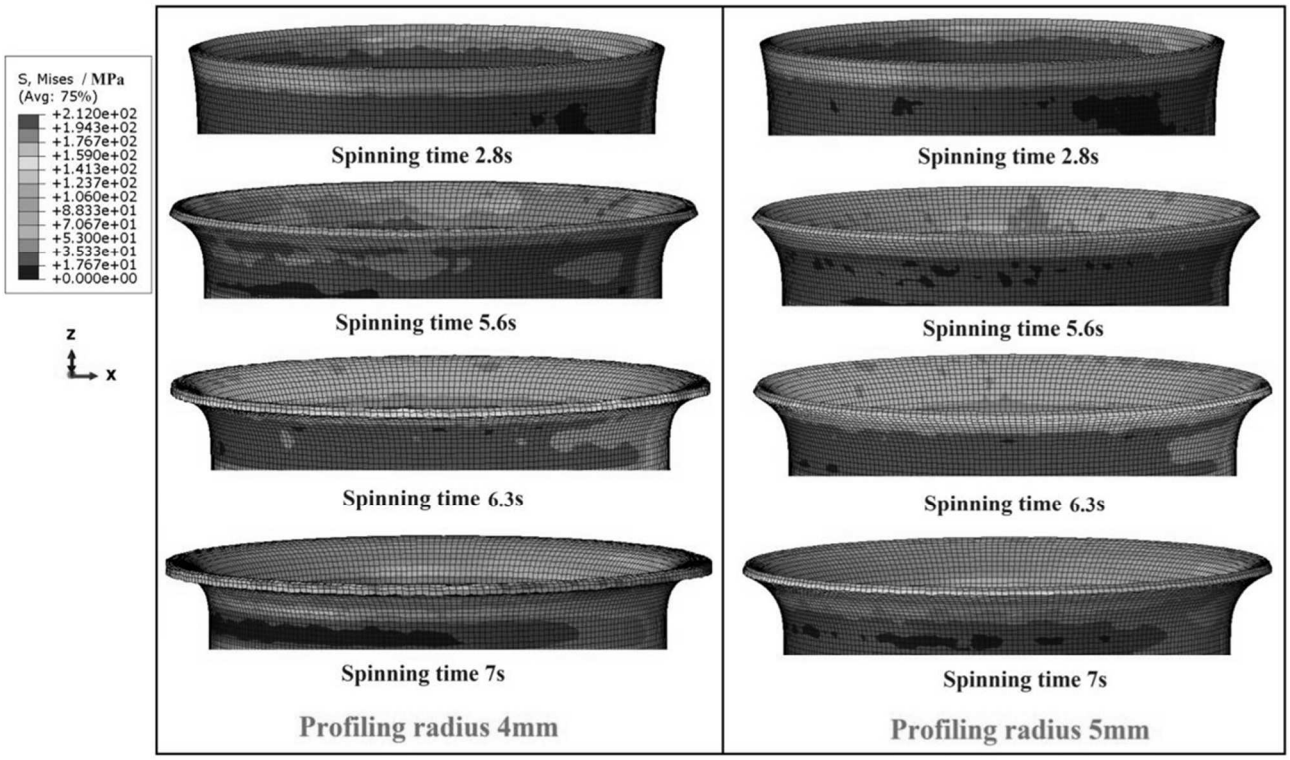

Fig. 4 *Mises stress during spinning process*

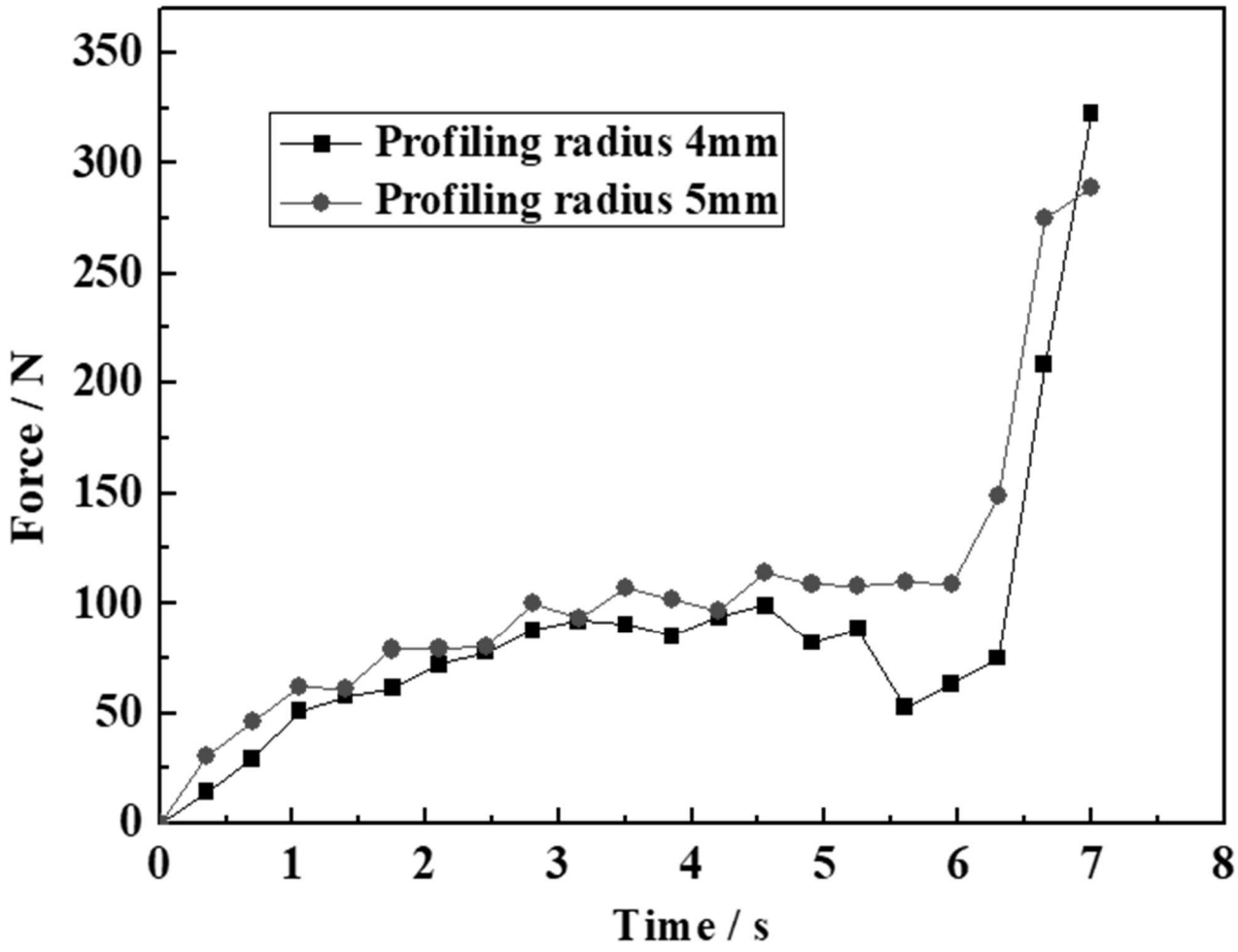

Fig. 5 *X-direction reaction force on the roller*

3.3 Strain and wall thickness

Fig. 6 shows the distribution of the equivalent strain on the spun outer flange during the spinning process. Before the spinning time of 5.6 s, the equivalent strain on deforming zone of the workpieces with the two radii is almost the same due to the bigger x-direction displacement of the material which does not adhere to the roller during this period. When the spinning time comes to 6.3 s, the larger contour curvature limits the flow space of the metal in the Z direction, resulting in a much greater force in the Z direction than in conditions with smaller curvature. So the larger forming force causes the blank to have greater overall deformation until the end of spinning process.

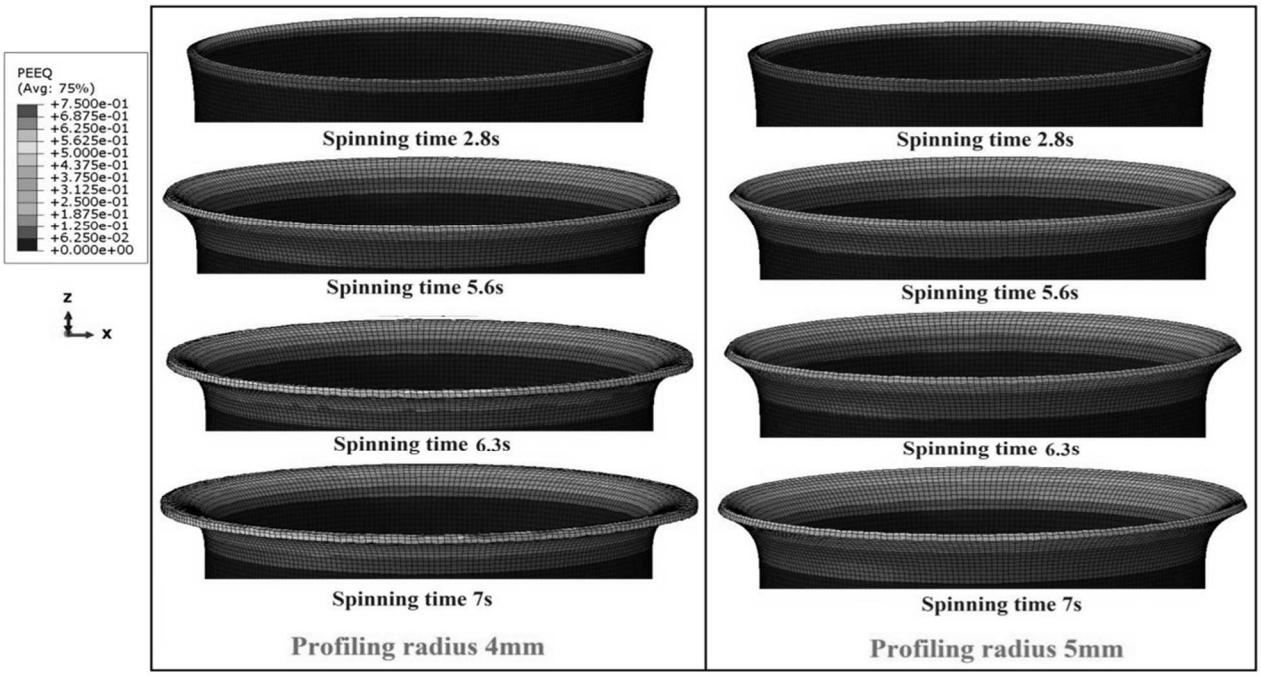

Fig. 6 *Equivalent strain during spinning process*

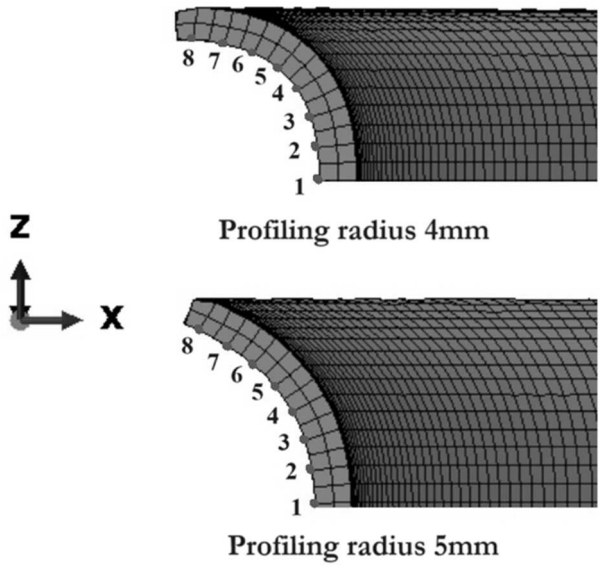

Fig. 7 *Wall thickness measurement points*

8 points evenly arranged on the deformation area of the spun-outer flange have been selected for the wall thickness testing as shown in Fig. 7. and Fig. 8 shows the wall thickness testing value. I can be found that, the wall thickness value is close to or slightly bigger than the initial wall thickness of the blank (1mm) at the connection between the deformation and the non deformation zone, and then the wall thickness distribution shows a downward trend along the positive direction of the Z coordinate (negative direction of the X coordinate, in Fig.6). And the maximum reduction is about 10%, and the overall wall thickness with the 4mm profiling radius is slightly greater than that of the 5 mm one. However, the 5 mm-radius working condition has bigger wall thickness at the end of the outer flange.

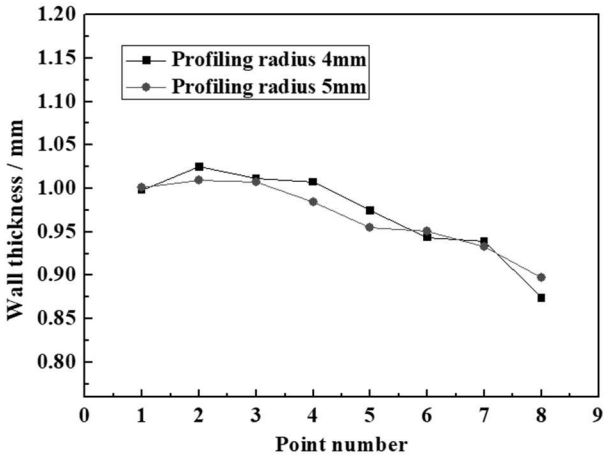

Fig. 8 *Wall thickness distribution*

The relationship between the wall thickness before and after spinning can be obtained through the principle of volume invariance in plastic deformation. The surface area on a cylindrical blank before being spun is calculated as Eq. (2).

$$S_0 = 2\pi R_p \ (D_0 + 2t_0) \quad (2)$$

Where:

R_p...The hight of the cylindrical blank involved in deformation, and it is theoretically equal to the profiling radius of the roller as show in Fig.2 [mm],

D_0...The inner diameter of the cylinder blank,

t_0…The wall thickness of the cylinder blank [mm].

The surface after outer flanging spinning is equivalent to a local circular ring surface, and can be calculated by using Eq. (3), assuming uniform spun wall thickness.

$$\begin{aligned} S_1 &= \int_0^{R_p} 2\pi (D_0 + 2t_1 + 2(R_p - \sqrt{R_p^2 - h^2})) \, dh \\ &= \int_0^{R_p} 2\pi (D_0 + 2t_1 + 2R_p) \, dh - \int_0^{R_p} 4\pi \sqrt{R_p^2 - h^2}) \, dh \\ &= 2\pi R_p \ (D_0 + 2t_1 + 2R_p) - 2\pi \ (R_p^2 \arcsin \frac{R_p}{R_p}) \\ &= 2\pi R_p \ (D_0 + 2t_1 + 2R_p) - \pi^2 R_p^2 \end{aligned} \quad (3)$$

Where:

t_1...The wall thickness of the spun outer flange [mm].

For thin-walled structures, their volume is approximated as surface area multiplied by wall thickness. Therefore Eq.(4) can be got, and the relationship between t_0 and t_1 is expressed as Eq. (5). By inputting the value of R_p, D_0, and t_0, it can be found that the theoretical calculated wall thickness values (t_1= 0.961 mm with 4 mm profiling radius; t_1= 0.951 mm with 5mm profiling radius) after spinning are basically consistent with the wall thickness values obtained by finite element analysis.

$$t_0 S_0 = t_1 S_1 \quad (4)$$

$$t_0 2\pi R_p \ (D_0 + 2t_0) = t_1 (2\pi R_p \ (D_0 + 2t_1 + 2R_p) - \pi^2 R_p^2) \quad (5)$$

4 Conclusion

The cylindrical outer flanging spinning is studied through the finite element modeling. The simulation results of deforming process, stress, strain and wall thickness are analyzed, and following conclusions are obtained:

- (1) A gap between the contour of the profiling roller and the blank exists until 1.5s before the end of the outer flanging spinning process. It is more unfavorable for the material to flow towards the roller with a larger curvature of the flange (with a smaller profiling radius), resulting in a time lag for the material to fully adhere to the roller.
- (2) The stress on the deforming zone is closely related to the contact area between the roller profile and the spun flange. The stress on the deformation zone of the larger flanging-curvature working condition is less than that of the smaller one before the blank and the roller fully adhere to.
- (3) Due to the fact that the surface area of the spun outer flange is larger than its original outer cylindrical surface, the formed wall thickness is slightly smaller than the initial wall thickness of the blank. Before the blank is completely aligned with the roller profile, the deformation of the 4mm flange radius spun workpiece is almost the same as that of 5mm one. After the metal is aligned with the roller, the deformation of the 4mm working condition is significantly greater than that of 5mm.

Acknowledgement

This work was supported by the National Natural Science Foundation, China (No. 52275355), Liaoning Provincial Department of Education Fund, China (No. JYTMS20230252) and the fundamental research funds for the universities of Liaoning province (No. LJ212410143083).

References

[1] XIA, Q., XIAO, G., LONG, H., CHENG, X., SHENG, X. (2014). A review of process advancement of novel metal spinning. In: *International Journal of Machine Tools and Manufacture*, Vol. 85, No. 7, pp. 100 – 121. ISSN: 0890-6955

[2] MUSIC, O., ALLWOOD, J.M., KAWAI, K. (2010). A review of the mechanics of metal spinning. In: *Journal of Materials Processing and Technology*, Vol. 210, No. 1, pp. 3–23. ISSN: 0924-0136

[3] WONG, C., DEAN, T.A., LIN, J. (2003). A review of spinning, shear forming and flow forming processes. In: *International Journal of Machine Tools and Manufacture*, Vol. 43, No. 14, pp. 1419–1435. ISSN: 0890 – 6955

[4] YUAN, Y., XIA, Q., XIAO, G., YANG, C. (2014) Experimental research on spinning forming of large slenderness ratio cylinders with different diameters. In: *Foging and stamping technology*, Vol. 49, No. 4, pp. 42 – 46. ISSN: 1000-3940 (in Chinese)

[5] HE, Z. (2017). Research on ball spinning flanging technology and design of special equipment [D]. Qihuang Dao: Yanshan university. (in Chinese)

[6] HUANG, S., HE, Z., WU, F., YANG, Y., WANG, X. (2018). Analysis on forming force of round hole flanging of ball spinning. In: Journal of plasticity engineering, Vol. 25, No. 5, pp. 217– 222. ISSN: 1007-2012 (in Chinese)

[7] XU, W., ZHANG, H., SHAN, D., GUO, B., KANG, D. (2008). Hot spinning technology of wheel rim of TC4 titanium alloy. In: *Materials science and technology*, Vol. 16, No. 1, pp. 14–18. ISSN: 1005-0299 (in Chinese)

[8] BAI, Q. (2016). Analysis of the power spinning made fanged bushing, In: *Bearing*, No. 11, pp. 28-32. ISSN: 1000–3762 (in Chinese)

[9] ZHAO, H., CAO, J., LIANG, B., SHUN, Z. (2020). Design and application of cylinder sleeve flanging spinning machine. In: *Metal Working: (Metal Cutting)*, No. 3, pp. 40–41. ISSN: 1674-1641 (in Chinese)

[10] JIA, Z., HAN, Z., LIU, B., FAN, Z. (2017). Numerical simulation and experimental study on the non-axisymmetric die-less shear spinning. In: *International Journal of Advanced Manufacturing Technology*, Vol. 92, No. 1-4, pp. 497–504. ISSN: 0268-3768

[11] XIA, Q., XIE, S., HUO, Y., RUAN, F. (2008). Numerical simulation and experimental research on the multi-pass neck-spinning of non-axisymmetric offset tube. In: *Journal of Materials Processing Technology*, Vol. 206, No. 1, pp. 500–508. ISSN: 0924-0136

[12] SUI, L., XIE, Y., LIU, B., JIA, Z. (2023). Finite element simulation of cylinder closure spinning. In: *Manufacturing Technology*, Vol. 23, No. 3, DOI: 10.21062/mft. 2023.040. ISSN: 1213-1489

[13] YE, T., JIA, Z., HAN, Z., XU, B., JI, S. (2020). Numerical simulation study on multi-pass non-axisymmetric spinning of cylindrical parts with oblique flange. In: *Proceedings of the institution of mechanical engineers part B-Journal of Engineering Manufacture*, Vol. 234, No. 1-2, pp. 75–83. ISSN: 0954-4054

[14] JIA, Z., HAN, Z., XU, Q., PENG, W., KONG, Q. (2015). Effects of processing parameters on the surface quality of square section die-less spinning. In: *International Journal of Advanced Manufacturing Technology*, Vol. 80, No. 9-12, pp. 1689–1700. ISSN: 0268-3768

[15] JIA, Z., HAN, Z., XU, Q., PENG, W. (2014). Numerical simulation and experiment study on hollow spinning process for square cross-section cone. In: *International Journal of Advanced Manufacturing Technology*, Vol. 75, No. 9-12, pp. 1605–1612. ISSN: 0268-3768